Searches for direct CP violation in two-body and quasi-two-body B meson decays at LHCb

Tom Hadavizadeh, University of Oxford
on behalf of the LHCb Collaboration

EPS-HEP 2019, Ghent, Belgium
10th - 17th July 2019

Introduction

- Direct CP asymmetries arise from interference between different amplitudes

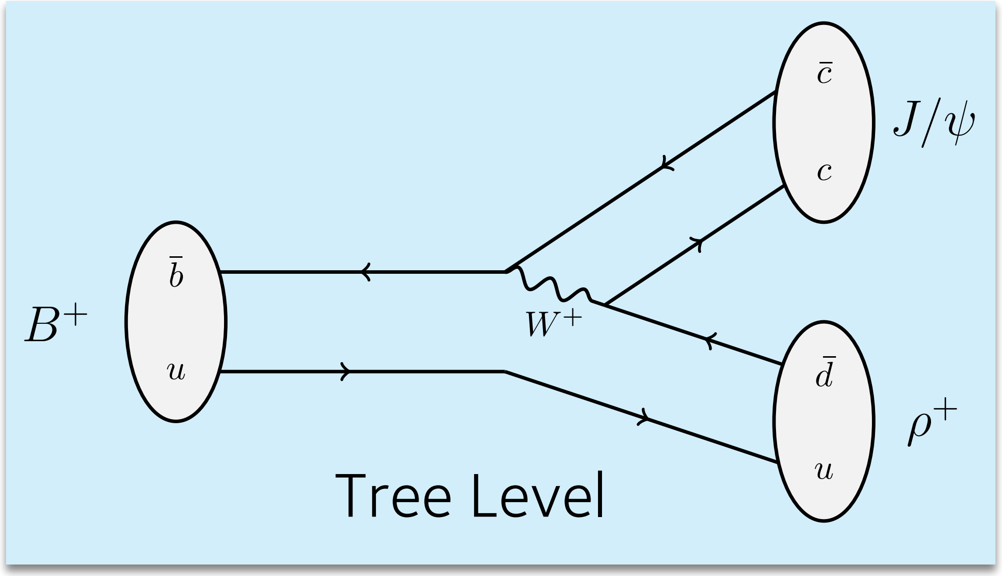

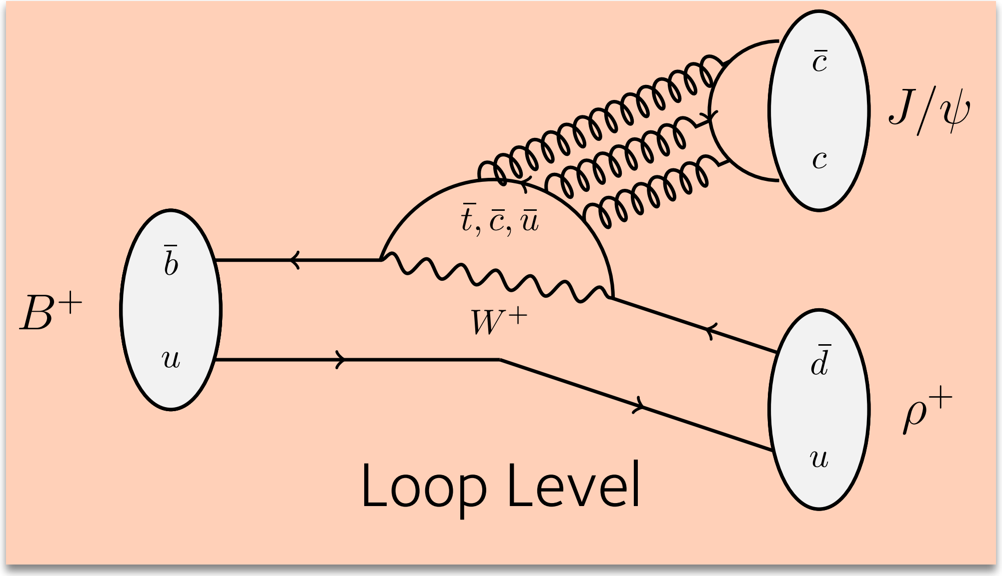

- The interference is largest when the competing amplitudes are of a similar size
- For suppressed decays, loop level processes can compete with tree level processes
- Decays with contributions from loop level amplitudes give access to processes beyond the standard model
- Heavy particles may produce effects that are observable with current sensitivities

Introduction

- This talk will cover three recent measurements of quasi-two-body decays with contributions from loop level processes

$$B^+ \to J/\psi \rho^+$$

🌳 + 🔄 + …

A measurement of direct CP asymmetry and branching fraction

$$B^0 \to \rho(770)^0 K^*(892)^0$$

🌳 + 🔄 + …

An amplitude analysis that determines CP asymmetries of contributing amplitudes

$$B^0_{(s)} \to K^{*0}\overline{K}^{*0}$$

🔄 + 🔄 + …

An amplitude analysis of a loop-mediated Flavour Changing Neutral Current process

All three analyses are performed using the 3 fb^{-1} Run 1 data set

Other talks

- Many other talks related to quasi-two-body decays are being presented by LHCb in this conference:

Time-dependent charmless B decays

$$B^0_{(s)} \to h^+ h'^-$$

including modes: $B^0_s \to (K^+\pi^-)(K^-\pi^+)$

$B^0_s \to \phi\phi$

Talk presented by Louis Henry
11:40 11th July

CP violation in multibody charmless b-hadron decays

Talk presented by Adam Morris
12:20 11th July

including modes: $B^0_s \to K^0_\mathrm{S} K^\pm \pi^\pm$

$B^\pm \to \pi^\pm K^+ K^-$

Observation of several sources of CP violation in $B^+ \to \pi^+ \pi^+ \pi^-$ decays at LHCb

Talk presented by Jeremy Dalseno
12:00 11th July

Recent results in quasi-two-body decays

LHCb-PAPER-2018-036
Eur. Phys. J. C79 (2019) 537

- Measurement of the branching fraction and CP asymmetry in $B^+ \rightarrow J/\psi\ \rho^+$ decays
- Study of the $B^0 \rightarrow \rho(770)^0\ K^*(892)^0$ decay with an amplitude analysis of $B^0 \rightarrow (\pi^+\pi^-)\ (K^-\pi^+)$
- Amplitude analysis of the $B_{(s)}{}^0 \rightarrow K^{*0}\ K^{*0}$ decays and measurement of the branching fraction of the $B^0 \rightarrow K^{*0}\ K^{*0}$ decay

$B^+ \to J/\psi\,\rho^+$

Run 1 3 fb^{-1}

- This decay process via tree and penguin topology processes

$$\mathcal{A}^{CP} \equiv \frac{\mathcal{B}(B^- \to J/\psi\,\rho^-) - \mathcal{B}(B^+ \to J/\psi\,\rho^+)}{\mathcal{B}(B^- \to J/\psi\,\rho^-) + \mathcal{B}(B^+ \to J/\psi\,\rho^+)}$$

- The value of A^{CP} provides an estimate of the penguin-to-tree amplitude ratio for b → $c\bar{c}d$ processes
- This can place constraints on penguin contributions in the determination of φ_s

(See talk by Veronika Chobanova)

Decays are reconstructed using three charged tracks and two photons

The branching fraction is measured relative to $B^+ \to J/\psi\,K^+$ decays

$$\begin{array}{l} B^+ \to J/\psi\rho^+ \\ \quad\quad\quad\quad \hookrightarrow \pi^+(\pi^0 \to \gamma\gamma) \\ \quad\quad \hookrightarrow \mu^+\mu^- \end{array}$$

Eur. Phys. J. C79 (2019) 537

$B^+ \to J/\psi\ \rho^+$

Selection

- Preselection
  - Kinematic, geometrical and vertex requirements

- Vetoes for specific backgrounds
  - Invariant mass vetoes remove $B^+ \to J/\psi\ \pi^+$ and $B^+ \to J/\psi\ K^+$ with a random π^0
  - Vertex quality requirements remove backgrounds with additional charged tracks

- Multi-variate analysis
  - A neural network is trained on simulations and data sidebands
  - Reweighing is used to ensure good data-MC agreement

- A kinematic fit is used to constrain the B^+ candidate to originate at the primary interaction, as well as the J/ψ and π^0 mass to known values

Eur. Phys. J. C79 (2019) 537

$B^+ \to J/\psi\, \rho^+$

Mass fit

- A 2D fit to $m(B^+)$ vs. $m(\rho^+)$ is performed, simultaneous for 2011 and 2012 data
- The production asymmetry of B^+ mesons determined in other measurements is subtracted $\mathcal{A}^{CP} = \mathcal{A}^{CP}_{\text{raw}} - \mathcal{A}^{\text{prod}}$

Results

- The results are the most precise to date

$$\mathcal{A}^{CP}(B^+ \to J/\psi\, \rho^+) = -0.045^{+0.056}_{-0.057} \pm 0.008$$
$$\mathcal{B}(B^+ \to J/\psi\, \rho^+) = (3.81^{+0.25}_{-0.24} \pm 0.35) \times 10^{-5}.$$

Systematics

- BF measurement is limited by π^0 reconstruction efficiency, dominated by BF($B^+ \to J/\psi\, K^{*+}$)

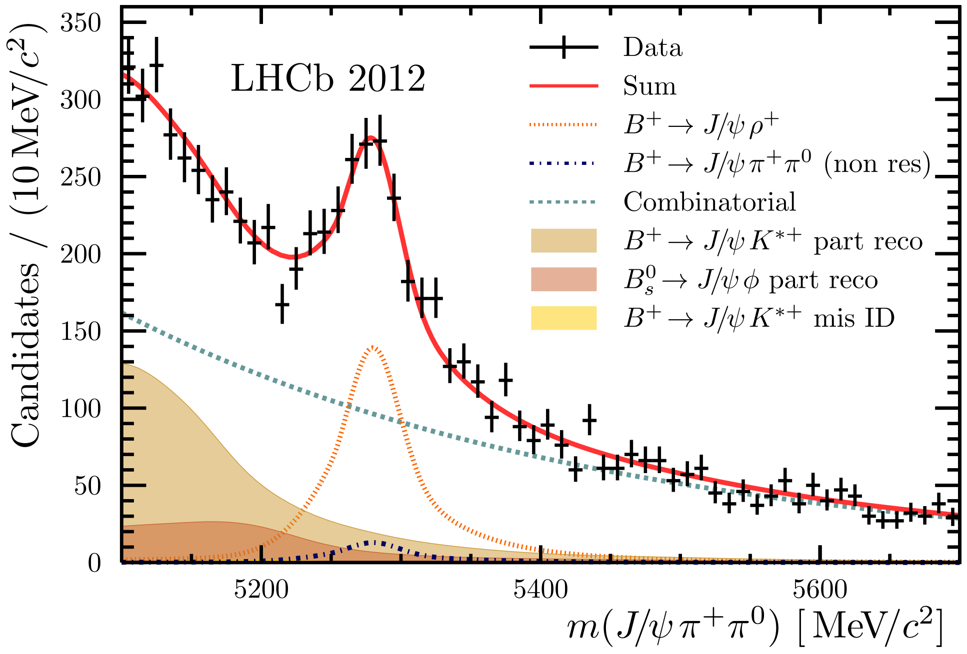

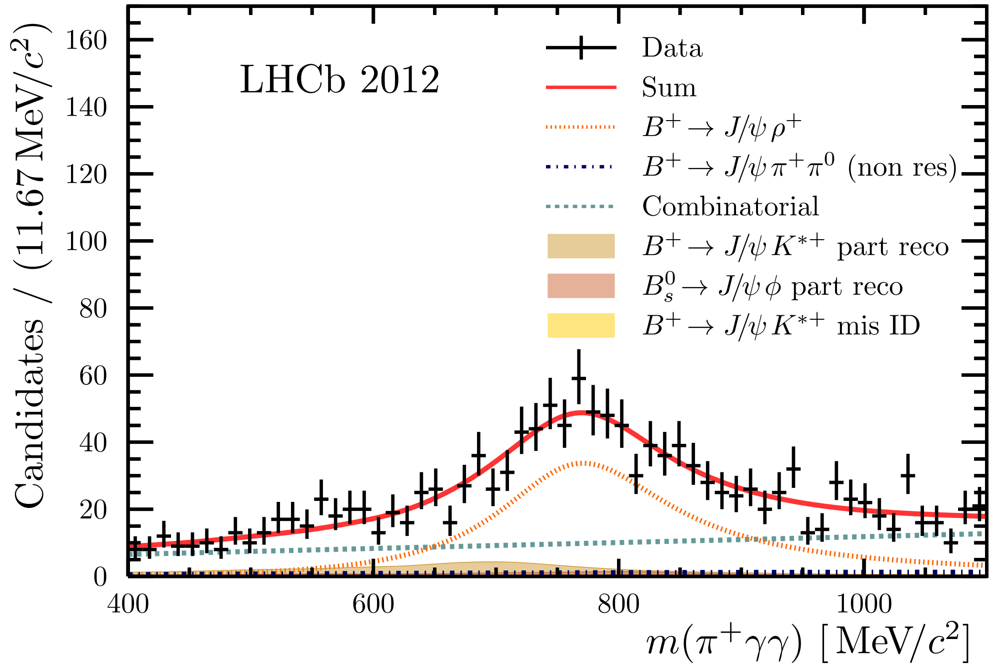

Eur. Phys. J. C79 (2019) 537

Recent results in quasi-two-body decays

- Measurement of the branching fraction and CP asymmetry in $B^+ \rightarrow J/\psi\ \rho^+$ decays

LHCb-PAPER-2018-042
JHEP 05 (2019) 026

- Study of the $B^0 \rightarrow \rho(770)^0\ K^*(892)^0$ decay with an amplitude analysis of $B^0 \rightarrow (\pi^+\pi^-)\ (K^-\pi^+)$

- Amplitude analysis of the $B_{(s)}{}^0 \rightarrow K^{*0}\ K^{*0}$ decays and measurement of the branching fraction of the $B^0 \rightarrow K^{*0}\ K^{*0}$ decay

$B^0 \rightarrow \rho^0 K^{*0}$

Run 1 3 fb^{-1}

$$B^0 \rightarrow (\pi^+\pi^-)(K^+\pi^-)$$

- Direct CP asymmetries are measured in this final state by determining the differences in partial widths of different amplitudes

$$B^0 \rightarrow \rho(770)^0 K^*(892)^0$$

- The tree-level contribution to this decay is doubly Cabibbo-suppressed so gluonic and electroweak penguins compete

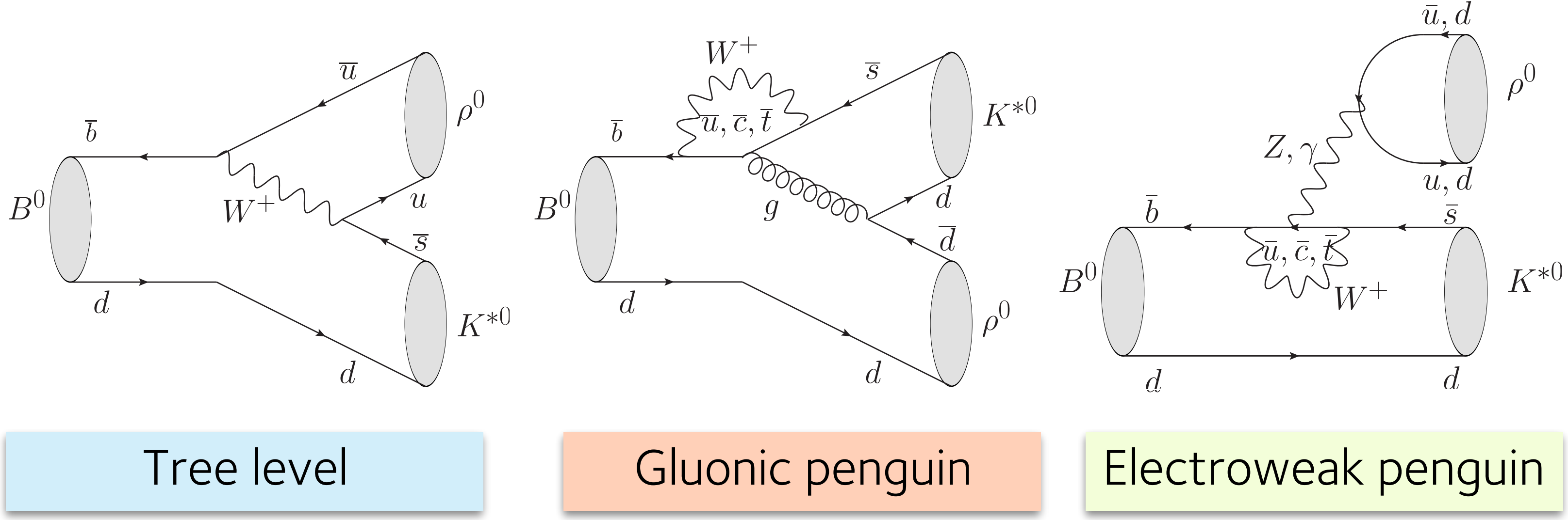

- In this P→VV decay, the electroweak penguin amplitudes contribute with different signs for different helicity eigenstates

JHEP 05 (2019) 026

$B^0 \rightarrow \rho^0 K^{*0}$

Selection

- **Preselection:** kinematic, geometric and particle identification requirements
- **Multi-variate analysis**
  - A BDT is trained on simulations and data side bands
- **Vetoes for specific backgrounds**
  - Particle identification requirements remove $\Lambda_b^0 \rightarrow p\pi\pi\pi$ decays
  - D^0 veto to remove incorrectly paired $B^0 \rightarrow D^0 \pi\pi$ decays
  - Three body modes including $B^0 \rightarrow D^- \pi^+$ removed with angular cut

Mass fit

- Data split into 8 simultaneous categories (trigger, year and charge)
- $B_s^0 \rightarrow (K\pi)(K\pi)$ background is subtracted by injecting simulations with negative weights
- sPlot method used to extract signal components

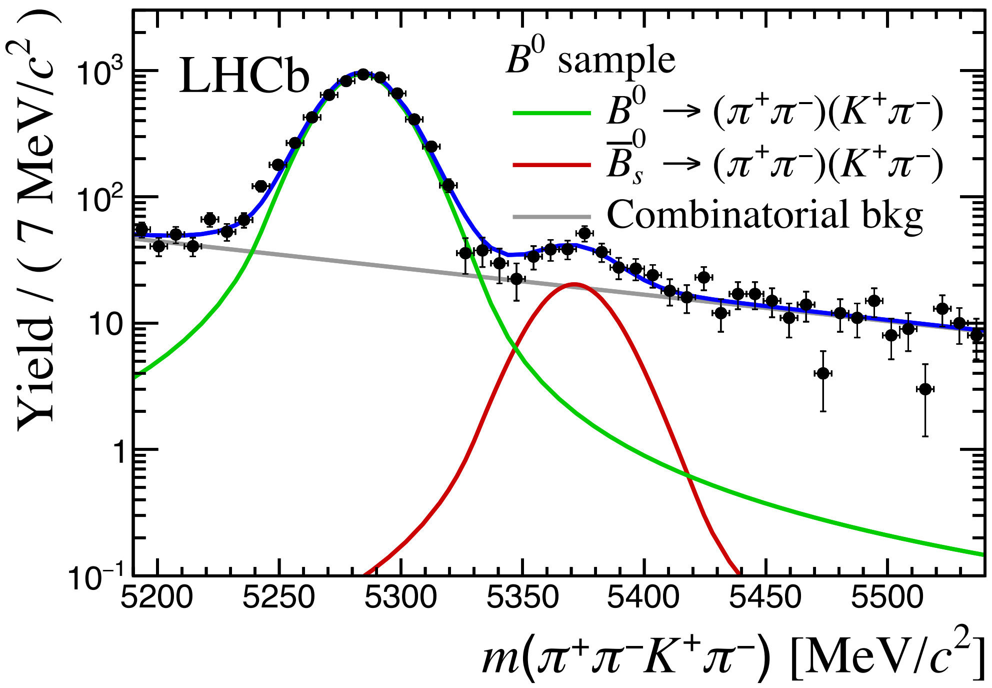

JHEP 05 (2019) 026

Amplitude model

- The amplitude model is made up from different contributions within the (ππ) and (Kπ) mass windows

		Kπ resonances	
		K*(892)^0	scalar Kπ
ππ resonances	ρ	VV	SV
	ω	VV	SV
	f$_0$(500)^0	SV	SS
	f$_0$(980)^0	SV	SS
	f$_0$(1370)^0	SV	SS

- Three helicity amplitudes contribute from each VV combination

- For VV amplitudes the polarisation fraction is defined to be:

$$f_{VV}^{0,\parallel,\perp} = \frac{|A_{VV}^{0,\parallel,\perp}|^2}{|A_{VV}^0|^2 + |A_{VV}^{\parallel}|^2 + |A_{VV}^{\perp}|^2}$$

- CP averages and asymmetries are constructed for particle and antiparticle decays

$$\tilde{f}_{VV} = \frac{1}{2}(f_{VV} + \overline{f}_{VV}) \qquad A_{VV} = \frac{\overline{f}_{VV} - f_{VV}}{\overline{f}_{VV} + f_{VV}}$$

- Additionally, phase differences and T-odd quantities are measured

JHEP 05 (2019) 026

Amplitude fit

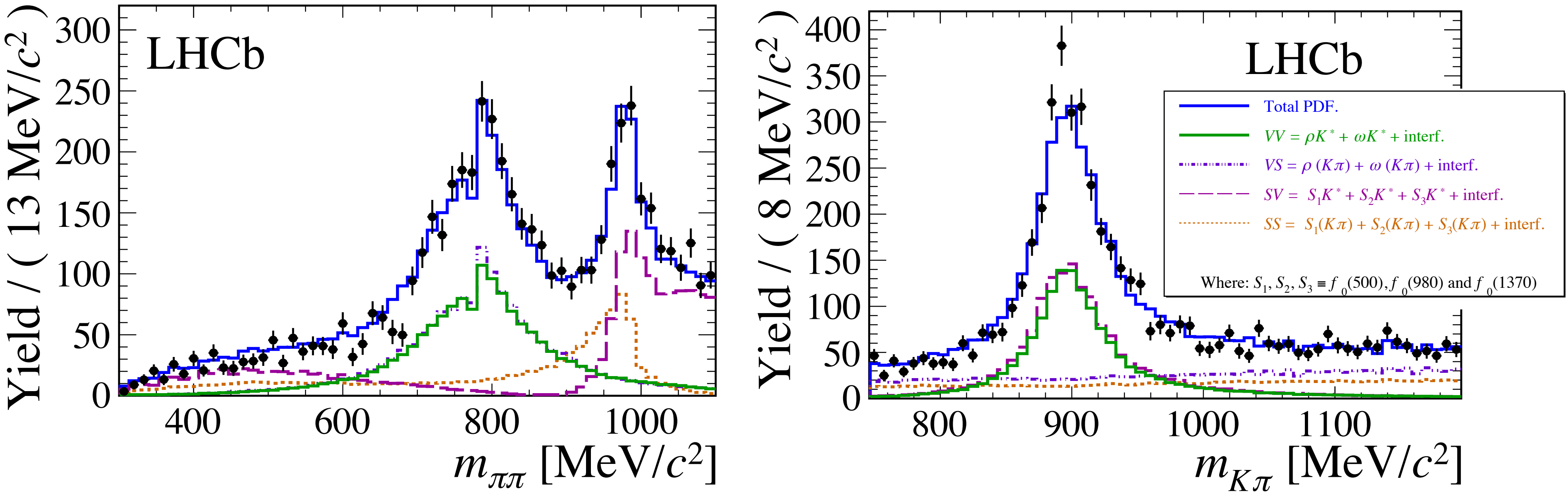

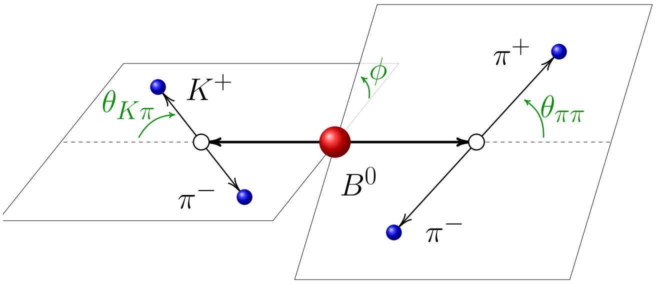

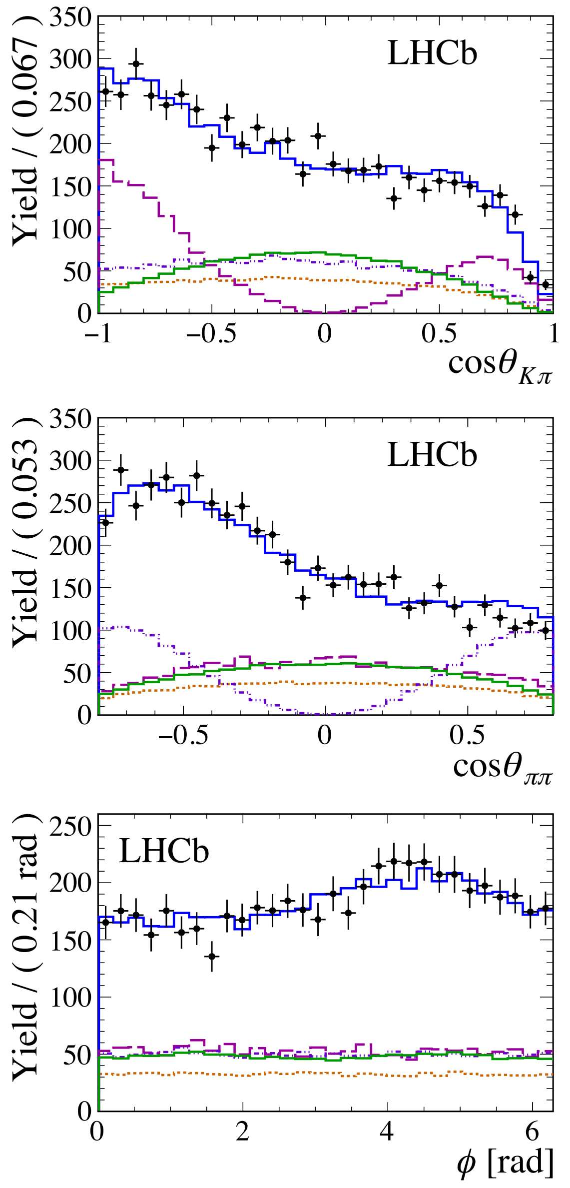

JHEP 05 (2019) 026

Results

- A small polarisation fraction and significant direct CP asymmetry is measured for the B⁰ → ρ⁰ K*⁰ component

$$\tilde{f}^{0}_{\rho K^*} = 0.164 \pm 0.015 \pm 0.022 \qquad \mathcal{A}^{0}_{\rho K^*} = -0.62 \pm 0.09 \pm 0.09$$

- This is the first observation of CP asymmetry in angular distributions of B⁰ → VV decays

Recent results in quasi-two-body decays

- Measurement of the branching fraction and CP asymmetry in $B^+ \rightarrow J/\psi\, \rho^+$ decays

- Study of the $B^0 \rightarrow \rho(770)^0 K^*(892)^0$ decay with an amplitude analysis of $B^0 \rightarrow (\pi^+\pi^-) (K^-\pi^+)$

LHCb-PAPER-2019-004
Submitted to JHEP

- Amplitude analysis of the $B_{(s)}{}^0 \rightarrow K^{*0} K^{*0}$ decays and measurement of the branching fraction of the $B^0 \rightarrow K^{*0} K^{*0}$ decay

B0 → K*0 $\overline{\text{K}}$*0

Run 1 3 fb-1

$$B^0_{(s)} \to (K^-\pi^+)(K^+\pi^-)$$

- This analysis performs an untagged, time-integrated amplitude analysis

$$B^0_s \to K^{*0}\overline{K}^{*0}$$

- Can be used to measure the unitarity angle β_s, relevant in B_s^0 processes
- High precision measurements require control of sub-leading amplitudes
- Previous measurement suggest no CP asymmetry, small polarisation fraction and small S-wave contribution

arXiv:1712.08683

$$B^0 \to K^{*0}\overline{K}^{*0}$$

- Flavour changing neutral current
- Helps control higher-order contributions to B_s^0 mode
- There is a 2.2 sigma difference between Belle and BaBar branching fraction measurements
- Both find large polarisation fraction

- This analysis updates polarisation fractions, S-wave contributions and measures B^0 branching fraction

arXiv:1905.06662

$B^0 \to K^{*0} \overline{K}^{*0}$

Selection

- **Preselection:**
  - Kinematic, geometrical and particle identification requirements
- **Multi-variate analysis:**
  - Gradient boosted BDT trained on MC and data sidebands
- **Vetoes for specific Backgrounds:**
  - Invariant mass windows and PID selections suppress many peaking backgrounds

Mass fit

- A simultaneous fit is performed to 2011 and 2012 data
- $B^0 \to \rho^0 K^{*0}$ background is subtracted by injecting simulations with negative weights
- sPlot method used to extract signal components

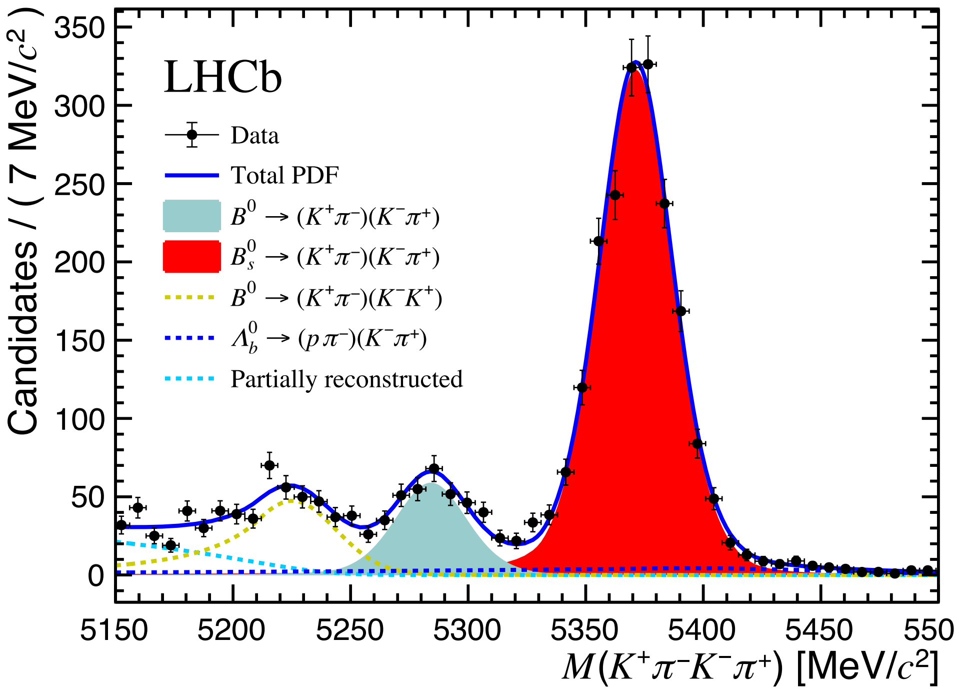

arXiv:1905.06662

Amplitude Model

- The amplitude model is made up from S-wave and P-wave Kπ resonances

$K^+\pi^-$ resonances

$K^-\pi^+$ resonances	$K^*(892)^0$	$K_0^*(1430)^0$	$K_0^*(700)^0$	$(K\pi)_0$
$K^*(892)^0$	VV	VS	VS	VS
$K_0^*(1430)^0$	SV	SS	SS	SS
$K_0^*(700)^0$	SV	SS	SS	SS
$(K\pi)_0$	SV	SS	SS	SS

- The polarisation fraction is measured for the VV contribution

$$f_{VV}^{0,\|,\perp} = \frac{|A_{VV}^{0,\|,\perp}|^2}{|A_{VV}^{0}|^2 + |A_{VV}^{\|}|^2 + |A_{VV}^{\perp}|^2}$$

- Additionally the S-wave fraction can be determined from the amplitudes of the SS, SV and VS contributions

arXiv:1905.06662

Amplitude fit

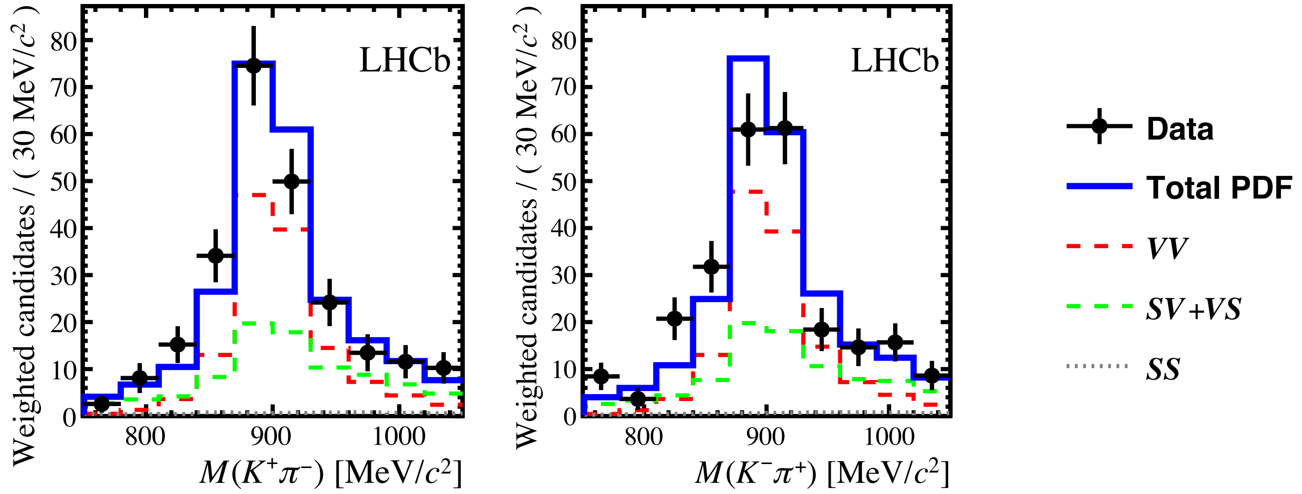

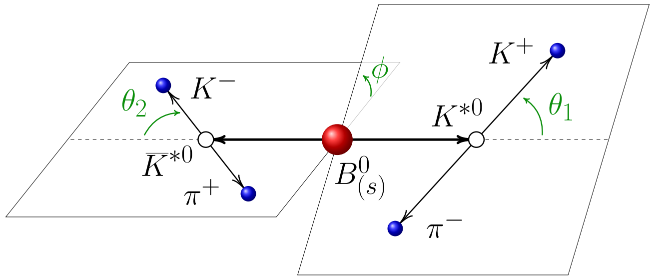

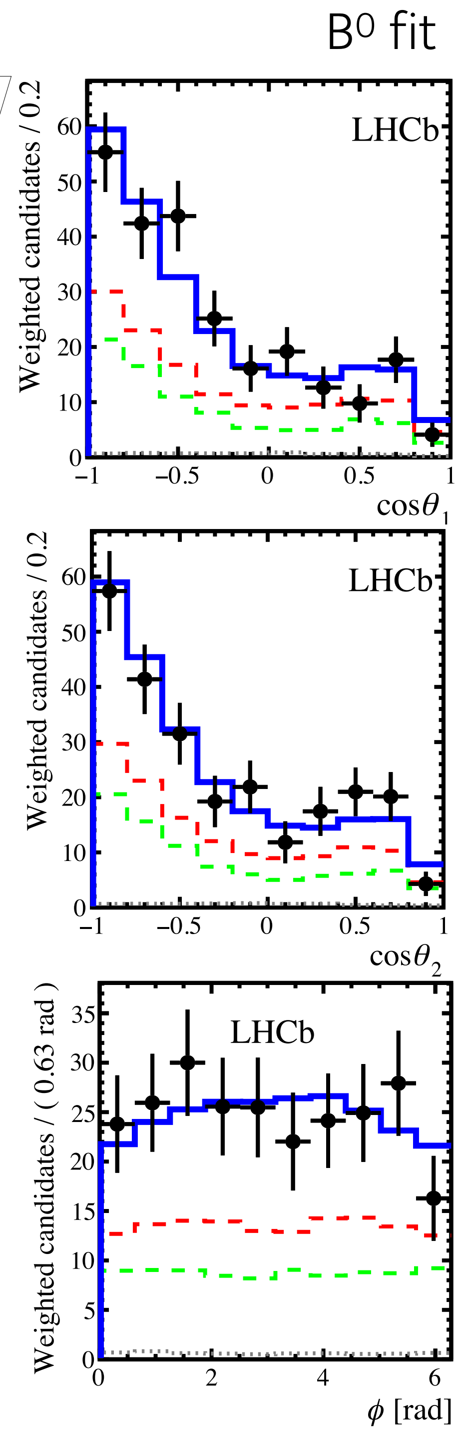

Results

- The longitudinal polarisation fractions confirm previous measurements

$$f_L(B^0) = 0.724 \pm 0.051 \pm 0.016$$
$$f_L(B^0_s) = 0.240 \pm 0.031 \pm 0.025$$

- The branching fraction of $B^0 \rightarrow K^{*0}\overline{K}^{*0}$ decays is determined to be

$$\mathcal{B}(B^0 \to K^{*0}\overline{K}^{*0}) = (8.0 \pm 0.9\,(\text{stat}) \pm 0.4\,(\text{syst})) \times 10^{-7}$$

Belle $\mathcal{B} = 2.6^{+3.3+1.0}_{-2.9-0.7} \times 10^{-7}$ Phys. Rev. D81 (2010) 071101

BaBar $\mathcal{B} = 12.8^{+3.5}_{-3.0} \times 10^{-7}$ Phys. Rev. Lett. 100 (2008) 081801

arXiv:1905.06662

Summary

- LHCb has produced measurements of CP asymmetries, branching fractions and polarisation fractions in quasi-two-body decays including:

The most precise measurement of CP asymmetry and branching fraction of $B^+ \rightarrow J/\psi\, \rho^+$ decays

This is the first observation of CP asymmetry in angular distributions of $B^0 \rightarrow \rho^0 K^{*0}$ decays

Polarisation fraction and branching fraction measurements in $B^0 \rightarrow K^{*0} \overline{K}^{*0}$ decays

- LHCb has a large sample of Run 2 data, so expect more exciting results in the near future

Back Up

$B^+ \rightarrow J/\psi\, \rho^+$

Branching fraction systematics

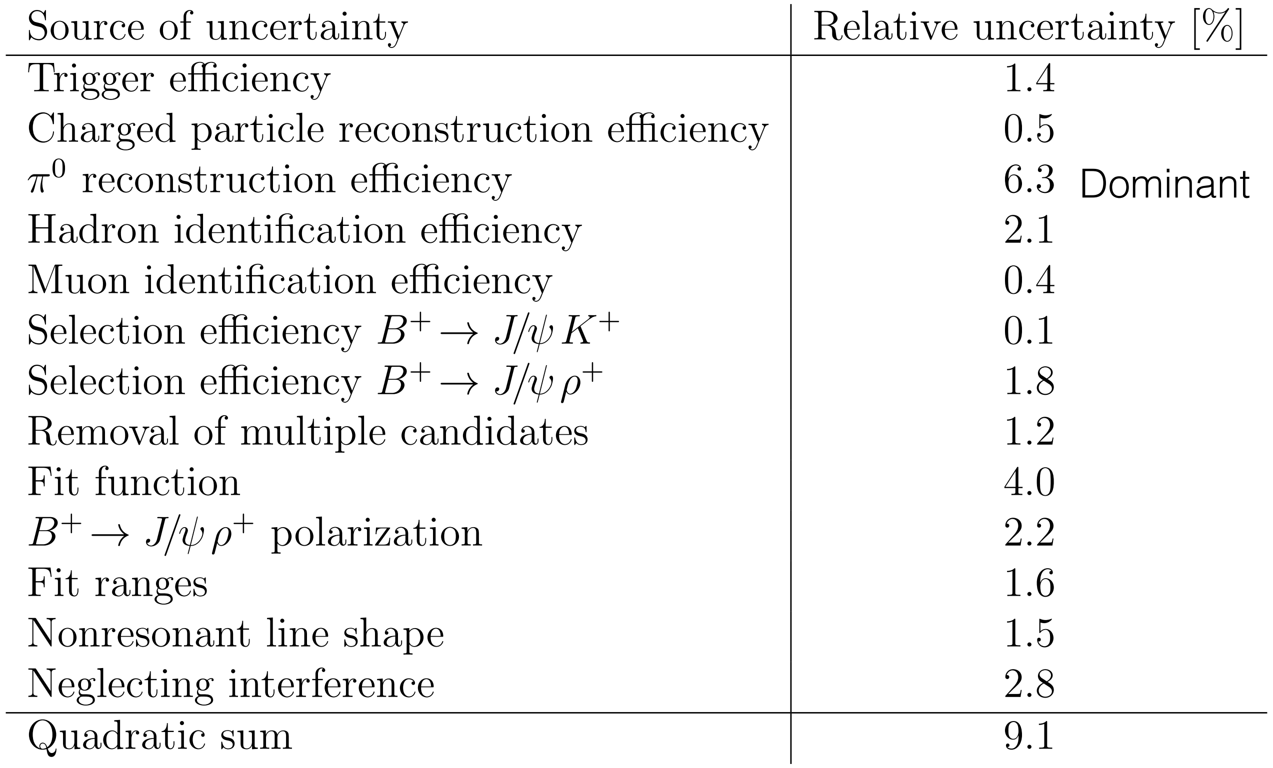

Source of uncertainty	Relative uncertainty [%]
Trigger efficiency	1.4
Charged particle reconstruction efficiency	0.5
π^0 reconstruction efficiency	6.3 Dominant
Hadron identification efficiency	2.1
Muon identification efficiency	0.4
Selection efficiency $B^+ \rightarrow J/\psi\, K^+$	0.1
Selection efficiency $B^+ \rightarrow J/\psi\, \rho^+$	1.8
Removal of multiple candidates	1.2
Fit function	4.0
$B^+ \rightarrow J/\psi\, \rho^+$ polarization	2.2
Fit ranges	1.6
Nonresonant line shape	1.5
Neglecting interference	2.8
Quadratic sum	9.1

A_{CP} systematics

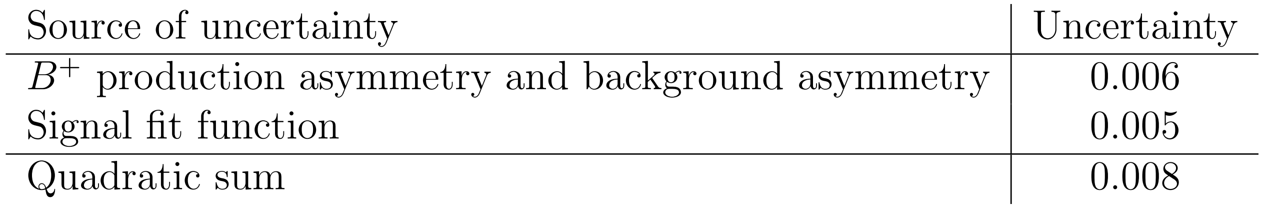

Source of uncertainty	Uncertainty
B^+ production asymmetry and background asymmetry	0.006
Signal fit function	0.005
Quadratic sum	0.008

$B^+ \rightarrow J/\psi\ \rho^+$

Mass fit

- Shapes:
  - Signal B+ mass: Sum of two Crystal Ball functions with tails fixed from simulation
  - Signal rho+ mass: Relativistic Breit-Wigner with parameters fixed to simulation
  - Part-Reco: two-dimensional kernel density estimations

$B^0 \to \rho^0 K^{*0}$

Full results

Parameter	CP average, $\tilde{f}$	CP asymmetry, $\mathcal{A}$
$\lvert A^0_{\rho K^*}\rvert^2$	$0.32 \pm 0.04 \pm 0.07$	$-0.75 \pm 0.07 \pm 0.17$
$\lvert A^{\lVert}_{\rho K^*}\rvert^2$	$0.70 \pm 0.04 \pm 0.08$	$-0.049 \pm 0.053 \pm 0.019$
$\lvert A^{\perp}_{\rho K^*}\rvert^2$	$0.67 \pm 0.04 \pm 0.07$	$-0.187 \pm 0.051 \pm 0.026$
$\lvert A^0_{\omega K^*}\rvert^2$	$0.019 \pm 0.010 \pm 0.012$	$-0.6 \pm 0.4 \pm 0.4$
$\lvert A^{\lVert}_{\omega K^*}\rvert^2$	$0.0050 \pm 0.0029 \pm 0.0031$	$-0.30 \pm 0.54 \pm 0.28$
$\lvert A^{\perp}_{\omega K^*}\rvert^2$	$0.0020 \pm 0.0019 \pm 0.0015$	$-0.2 \pm 0.9 \pm 0.4$
$\lvert A_{\omega(K\pi)}\rvert^2$	$0.026 \pm 0.011 \pm 0.025$	$-0.47 \pm 0.33 \pm 0.45$
$\lvert A_{f_0(500)K^*}\rvert^2$	$0.53 \pm 0.05 \pm 0.10$	$-0.06 \pm 0.09 \pm 0.04$
$\lvert A_{f_0(980)K^*}\rvert^2$	$2.42 \pm 0.13 \pm 0.25$	$-0.022 \pm 0.052 \pm 0.023$
$\lvert A_{f_0(1370)K^*}\rvert^2$	$1.29 \pm 0.09 \pm 0.20$	$-0.09 \pm 0.07 \pm 0.04$
$\lvert A_{f_0(500)(K\pi)}\rvert^2$	$0.174 \pm 0.021 \pm 0.039$	$0.30 \pm 0.12 \pm 0.09$
$\lvert A_{f_0(980)(K\pi)}\rvert^2$	$1.18 \pm 0.08 \pm 0.07$	$-0.083 \pm 0.066 \pm 0.023$
$\lvert A_{f_0(1370)(K\pi)}\rvert^2$	$0.139 \pm 0.028 \pm 0.039$	$-0.48 \pm 0.17 \pm 0.15$
$f^0_{\rho K^*}$	$0.164 \pm 0.015 \pm 0.022$	$-0.62 \pm 0.09 \pm 0.09$
$f^{\lVert}_{\rho K^*}$	$0.435 \pm 0.016 \pm 0.042$	$0.188 \pm 0.037 \pm 0.022$
$f^{\perp}_{\rho K^*}$	$0.401 \pm 0.016 \pm 0.037$	$0.050 \pm 0.039 \pm 0.015$
$f^0_{\omega K^*}$	$0.68 \pm 0.17 \pm 0.16$	$-0.13 \pm 0.27 \pm 0.13$
$f^{\lVert}_{\omega K^*}$	$0.22 \pm 0.14 \pm 0.15$	$0.26 \pm 0.55 \pm 0.22$
$f^{\perp}_{\omega K^*}$	$0.10 \pm 0.09 \pm 0.09$	$0.3 \pm 0.8 \pm 0.4$

Parameter	CP average, $\frac{1}{2}(\delta_{\overline{B}} + \delta_B)$ [rad]	CP difference, $\frac{1}{2}(\delta_{\overline{B}} - \delta_B)$ [rad]
$\delta^0_{\rho K^*}$	$1.57 \pm 0.08 \pm 0.18$	$0.12 \pm 0.08 \pm 0.04$
$\delta^{\lVert}_{\rho K^*}$	$0.795 \pm 0.030 \pm 0.068$	$0.014 \pm 0.030 \pm 0.026$
$\delta^{\perp}_{\rho K^*}$	$-2.365 \pm 0.032 \pm 0.054$	$0.000 \pm 0.032 \pm 0.013$
$\delta^0_{\omega K^*}$	$-0.86 \pm 0.29 \pm 0.71$	$0.03 \pm 0.29 \pm 0.16$
$\delta^{\lVert}_{\omega K^*}$	$-1.83 \pm 0.29 \pm 0.32$	$0.59 \pm 0.29 \pm 0.07$
$\delta^{\perp}_{\omega K^*}$	$1.6 \pm 0.4 \pm 0.6$	$-0.25 \pm 0.43 \pm 0.16$
$\delta_{\omega(K\pi)}$	$-2.32 \pm 0.22 \pm 0.24$	$-0.20 \pm 0.22 \pm 0.14$
$\delta_{f_0(500)K^*}$	$-2.28 \pm 0.06 \pm 0.22$	$-0.00 \pm 0.06 \pm 0.05$
$\delta_{f_0(980)K^*}$	$0.39 \pm 0.04 \pm 0.07$	$0.018 \pm 0.038 \pm 0.022$
$\delta_{f_0(1370)K^*}$	$-2.76 \pm 0.05 \pm 0.09$	$0.076 \pm 0.051 \pm 0.025$
$\delta_{f_0(500)(K\pi)}$	$-2.80 \pm 0.09 \pm 0.21$	$-0.206 \pm 0.088 \pm 0.034$
$\delta_{f_0(980)(K\pi)}$	$-2.982 \pm 0.032 \pm 0.057$	$-0.027 \pm 0.032 \pm 0.013$
$\delta_{f_0(1370)(K\pi)}$	$1.76 \pm 0.10 \pm 0.11$	$-0.16 \pm 0.10 \pm 0.04$
$\delta^{\lVert-\perp}_{\rho K^*}$	$3.160 \pm 0.035 \pm 0.044$	$0.014 \pm 0.035 \pm 0.026$
$\delta^{\lVert-0}_{\rho K^*}$	$-0.77 \pm 0.09 \pm 0.06$	$-0.109 \pm 0.085 \pm 0.034$
$\delta^{\perp-0}_{\rho K^*}$	$-3.93 \pm 0.09 \pm 0.07$	$-0.123 \pm 0.085 \pm 0.035$
$\delta^{\lVert-\perp}_{\omega K^*}$	$-3.4 \pm 0.5 \pm 0.7$	$0.84 \pm 0.52 \pm 0.16$
$\delta^{\lVert-0}_{\omega K^*}$	$-1.0 \pm 0.4 \pm 0.6$	$0.57 \pm 0.41 \pm 0.17$
$\delta^{\perp-0}_{\omega K^*}$	$2.4 \pm 0.5 \pm 0.8$	$-0.28 \pm 0.51 \pm 0.24$

$B^0 \to \rho^0 K^{*0}$

Comparison to theory

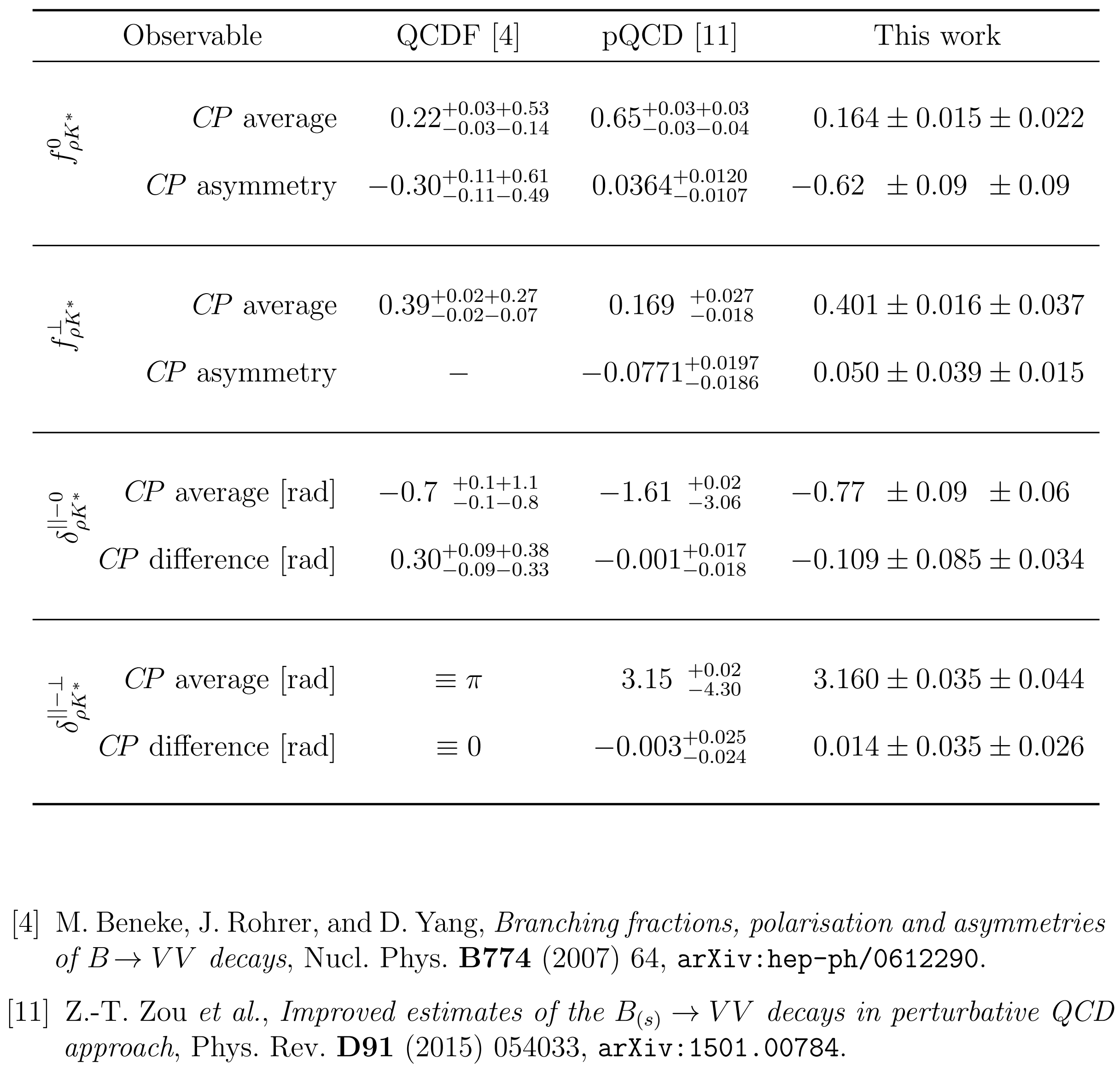

	Observable	QCDF [4]	pQCD [11]	This work
$f^0_{\rho K^*}$	*CP* average	$0.22^{+0.03+0.53}_{-0.03-0.14}$	$0.65^{+0.03+0.03}_{-0.03-0.04}$	$0.164 \pm 0.015 \pm 0.022$
	CP asymmetry	$-0.30^{+0.11+0.61}_{-0.11-0.49}$	$0.0364^{+0.0120}_{-0.0107}$	$-0.62 \pm 0.09 \pm 0.09$
$f^\perp_{\rho K^*}$	*CP* average	$0.39^{+0.02+0.27}_{-0.02-0.07}$	$0.169^{+0.027}_{-0.018}$	$0.401 \pm 0.016 \pm 0.037$
	CP asymmetry	–	$-0.0771^{+0.0197}_{-0.0186}$	$0.050 \pm 0.039 \pm 0.015$
$\delta^{\parallel-0}_{\rho K^*}$	*CP* average [rad]	$-0.7^{+0.1+1.1}_{-0.1-0.8}$	$-1.61^{+0.02}_{-3.06}$	$-0.77 \pm 0.09 \pm 0.06$
	CP difference [rad]	$0.30^{+0.09+0.38}_{-0.09-0.33}$	$-0.001^{+0.017}_{-0.018}$	$-0.109 \pm 0.085 \pm 0.034$
$\delta^{\parallel-\perp}_{\rho K^*}$	*CP* average [rad]	$\equiv \pi$	$3.15^{+0.02}_{-4.30}$	$3.160 \pm 0.035 \pm 0.044$
	CP difference [rad]	$\equiv 0$	$-0.003^{+0.025}_{-0.024}$	$0.014 \pm 0.035 \pm 0.026$

[4] M. Beneke, J. Rohrer, and D. Yang, *Branching fractions, polarisation and asymmetries of $B \to VV$ decays*, Nucl. Phys. **B774** (2007) 64, `arXiv:hep-ph/0612290`.

[11] Z.-T. Zou *et al.*, *Improved estimates of the $B_{(s)} \to VV$ decays in perturbative QCD approach*, Phys. Rev. **D91** (2015) 054033, `arXiv:1501.00784`.

Systematic uncertainties

- Uncertainties on the parameters in the mass propagators
- Angular momentum barrier factors
- Background subtractions
- Description of the kinematic acceptance
- Masses and angular resolution
- Fit method
- Pollution due to $B^0 \rightarrow a_1(1260)^- K^+$ decays
- Symmetrised $(\pi\pi)$ contributions in the model
- Simulation corrections

$B^0 \to \rho^0 K^{*0}$

Systematic uncertainties

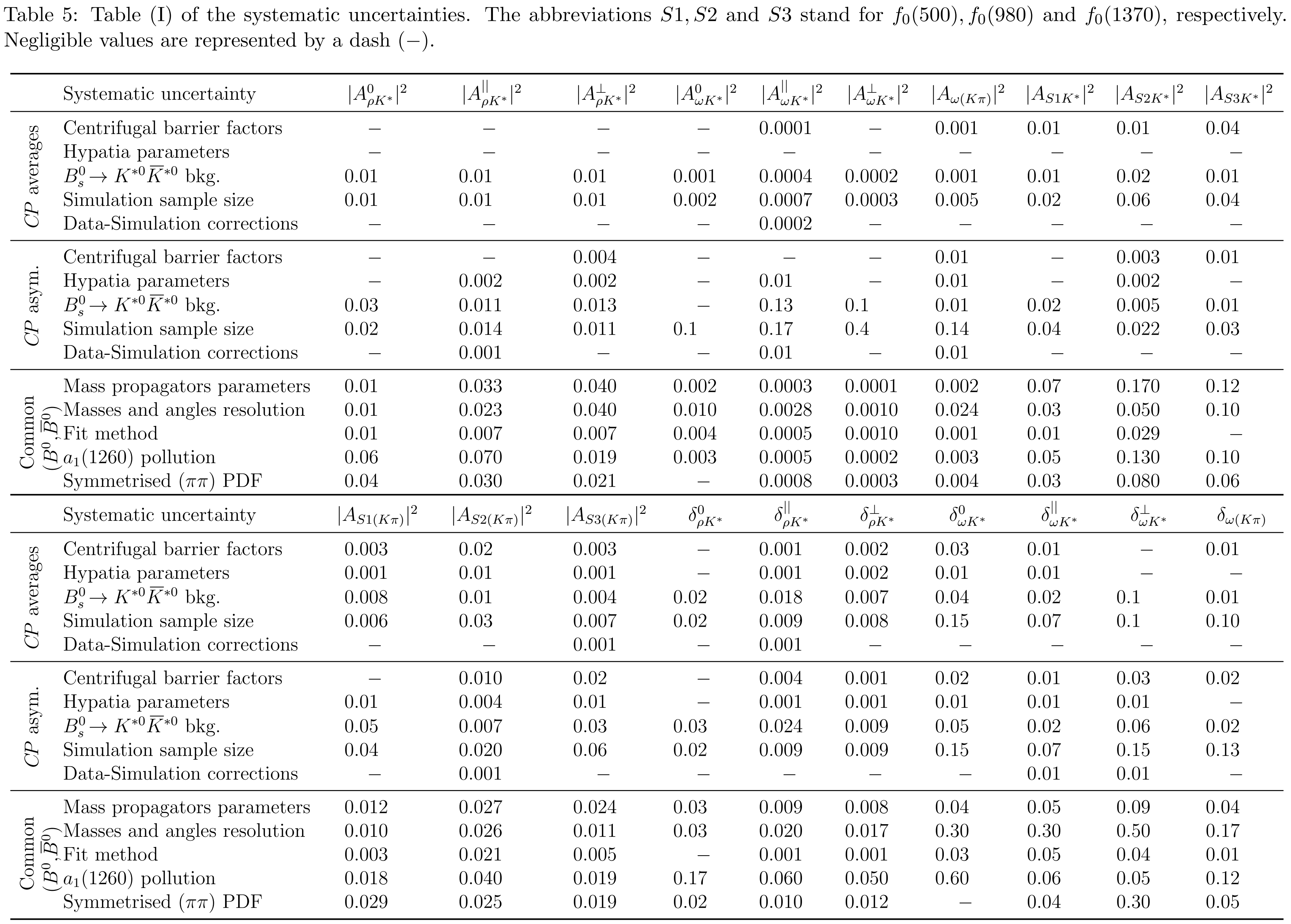

Table 5: Table (I) of the systematic uncertainties. The abbreviations $S1, S2$ and $S3$ stand for $f_0(500), f_0(980)$ and $f_0(1370)$, respectively. Negligible values are represented by a dash (–).

	Systematic uncertainty	$\lvert A^0_{\rho K^*}\rvert^2$	$\lvert A^{\vert\vert}_{\rho K^*}\rvert^2$	$\lvert A^{\perp}_{\rho K^*}\rvert^2$	$\lvert A^0_{\omega K^*}\rvert^2$	$\lvert A^{\vert\vert}_{\omega K^*}\rvert^2$	$\lvert A^{\perp}_{\omega K^*}\rvert^2$	$\lvert A_{\omega(K\pi)}\rvert^2$	$\lvert A_{S1K^*}\rvert^2$	$\lvert A_{S2K^*}\rvert^2$	$\lvert A_{S3K^*}\rvert^2$
CP averages	Centrifugal barrier factors	–	–	–	–	0.0001	–	0.001	0.01	0.01	0.04
	Hypatia parameters	–	–	–	–	–	–	–	–	–	–
	$B^0_s \to K^{*0}\overline{K}^{*0}$ bkg.	0.01	0.01	0.01	0.001	0.0004	0.0002	0.001	0.01	0.02	0.01
	Simulation sample size	0.01	0.01	0.01	0.002	0.0007	0.0003	0.005	0.02	0.06	0.04
	Data-Simulation corrections	–	–	–	–	0.0002	–	–	–	–	–
CP asym.	Centrifugal barrier factors	–	–	0.004	–	–	–	0.01	–	0.003	0.01
	Hypatia parameters	–	0.002	0.002	–	0.01	–	0.01	–	0.002	–
	$B^0_s \to K^{*0}\overline{K}^{*0}$ bkg.	0.03	0.011	0.013	–	0.13	0.1	0.01	0.02	0.005	0.01
	Simulation sample size	0.02	0.014	0.011	0.1	0.17	0.4	0.14	0.04	0.022	0.03
	Data-Simulation corrections	–	0.001	–	–	0.01	–	0.01	–	–	–
Common $(B^0, \overline{B}^0)$	Mass propagators parameters	0.01	0.033	0.040	0.002	0.0003	0.0001	0.002	0.07	0.170	0.12
	Masses and angles resolution	0.01	0.023	0.040	0.010	0.0028	0.0010	0.024	0.03	0.050	0.10
	Fit method	0.01	0.007	0.007	0.004	0.0005	0.0010	0.001	0.01	0.029	–
	$a_1(1260)$ pollution	0.06	0.070	0.019	0.003	0.0005	0.0002	0.003	0.05	0.130	0.10
	Symmetrised $(\pi\pi)$ PDF	0.04	0.030	0.021	–	0.0008	0.0003	0.004	0.03	0.080	0.06

	Systematic uncertainty	$\lvert A_{S1(K\pi)}\rvert^2$	$\lvert A_{S2(K\pi)}\rvert^2$	$\lvert A_{S3(K\pi)}\rvert^2$	$\delta^0_{\rho K^*}$	$\delta^{\vert\vert}_{\rho K^*}$	$\delta^{\perp}_{\rho K^*}$	$\delta^0_{\omega K^*}$	$\delta^{\vert\vert}_{\omega K^*}$	$\delta^{\perp}_{\omega K^*}$	$\delta_{\omega(K\pi)}$
CP averages	Centrifugal barrier factors	0.003	0.02	0.003	–	0.001	0.002	0.03	0.01	–	0.01
	Hypatia parameters	0.001	0.01	0.001	–	0.001	0.002	0.01	0.01	–	–
	$B^0_s \to K^{*0}\overline{K}^{*0}$ bkg.	0.008	0.01	0.004	0.02	0.018	0.007	0.04	0.02	0.1	0.01
	Simulation sample size	0.006	0.03	0.007	0.02	0.009	0.008	0.15	0.07	0.1	0.10
	Data-Simulation corrections	–	–	0.001	–	0.001	–	–	–	–	–
CP asym.	Centrifugal barrier factors	–	0.010	0.02	–	0.004	0.001	0.02	0.01	0.03	0.02
	Hypatia parameters	0.01	0.004	0.01	–	0.001	0.001	0.01	0.01	0.01	–
	$B^0_s \to K^{*0}\overline{K}^{*0}$ bkg.	0.05	0.007	0.03	0.03	0.024	0.009	0.05	0.02	0.06	0.02
	Simulation sample size	0.04	0.020	0.06	0.02	0.009	0.009	0.15	0.07	0.15	0.13
	Data-Simulation corrections	–	0.001	–	–	–	–	–	0.01	0.01	–
Common $(B^0, \overline{B}^0)$	Mass propagators parameters	0.012	0.027	0.024	0.03	0.009	0.008	0.04	0.05	0.09	0.04
	Masses and angles resolution	0.010	0.026	0.011	0.03	0.020	0.017	0.30	0.30	0.50	0.17
	Fit method	0.003	0.021	0.005	–	0.001	0.001	0.03	0.05	0.04	0.01
	$a_1(1260)$ pollution	0.018	0.040	0.019	0.17	0.060	0.050	0.60	0.06	0.05	0.12
	Symmetrised $(\pi\pi)$ PDF	0.029	0.025	0.019	0.02	0.010	0.012	–	0.04	0.30	0.05

$B^0 \to \rho^0 K^{*0}$

Systematic uncertainties

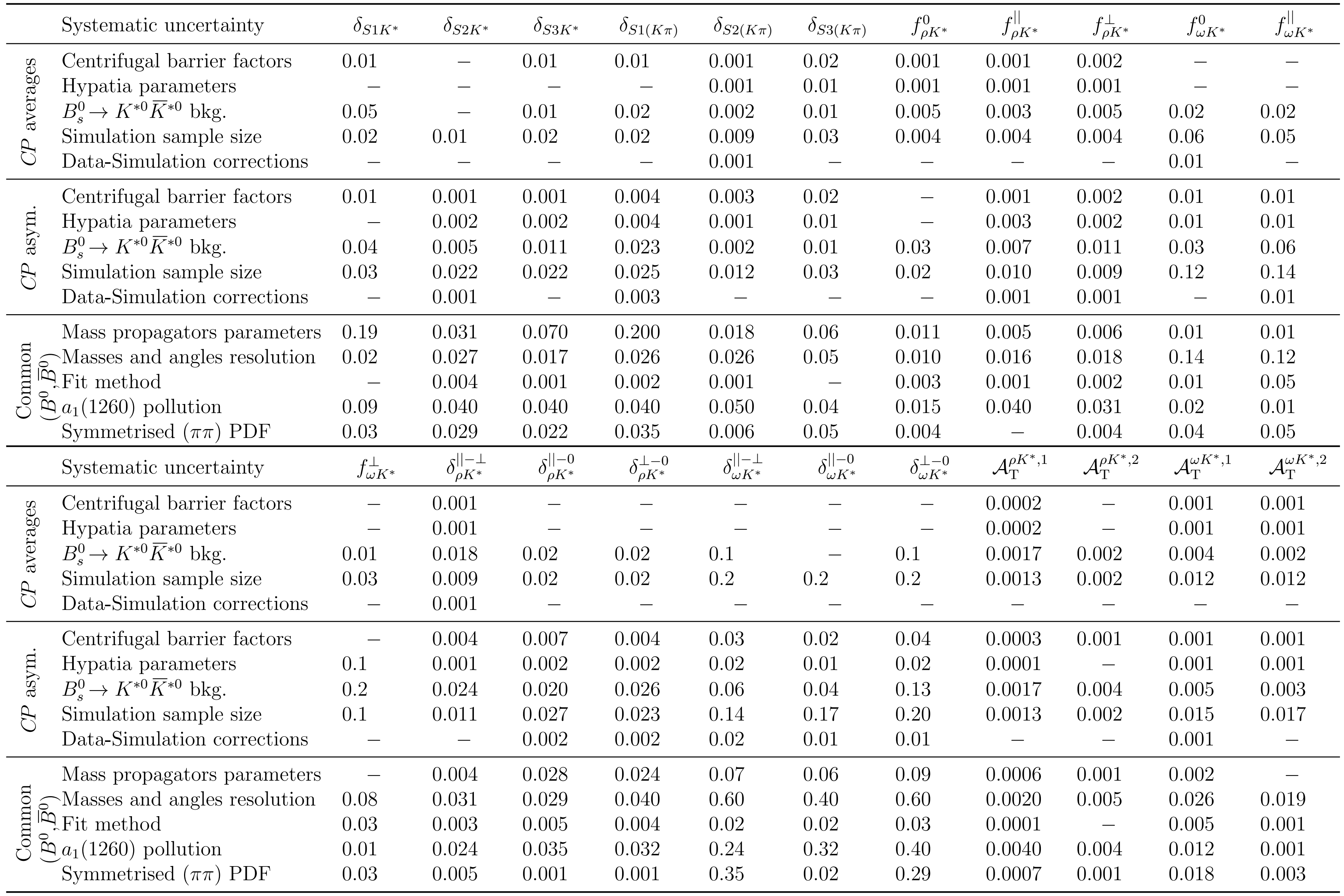

Table 6: Table (II) of the systematic uncertainties. The abbreviations $S1, S2$ and $S3$ stand for $f_0(500), f_0(980)$ and $f_0(1370)$, respectively. Negligible values are represented by a dash $(-)$.

	Systematic uncertainty	δ_{S1K^*}	δ_{S2K^*}	δ_{S3K^*}	$\delta_{S1(K\pi)}$	$\delta_{S2(K\pi)}$	$\delta_{S3(K\pi)}$	$f^0_{\rho K^*}$	$f^{\|\|}_{\rho K^*}$	$f^{\perp}_{\rho K^*}$	$f^0_{\omega K^*}$	$f^{\|\|}_{\omega K^*}$
CP averages	Centrifugal barrier factors	0.01	–	0.01	0.01	0.001	0.02	0.001	0.001	0.002	–	–
	Hypatia parameters	–	–	–	–	0.001	0.01	0.001	0.001	0.001	–	–
	$B^0_s \to K^{*0}\overline{K}^{*0}$ bkg.	0.05	–	0.01	0.02	0.002	0.01	0.005	0.003	0.005	0.02	0.02
	Simulation sample size	0.02	0.01	0.02	0.02	0.009	0.03	0.004	0.004	0.004	0.06	0.05
	Data-Simulation corrections	–	–	–	–	0.001	–	–	–	–	0.01	–
CP asym.	Centrifugal barrier factors	0.01	0.001	0.001	0.004	0.003	0.02	–	0.001	0.002	0.01	0.01
	Hypatia parameters	–	0.002	0.002	0.004	0.001	0.01	–	0.003	0.002	0.01	0.01
	$B^0_s \to K^{*0}\overline{K}^{*0}$ bkg.	0.04	0.005	0.011	0.023	0.002	0.01	0.03	0.007	0.011	0.03	0.06
	Simulation sample size	0.03	0.022	0.022	0.025	0.012	0.03	0.02	0.010	0.009	0.12	0.14
	Data-Simulation corrections	–	0.001	–	0.003	–	–	–	0.001	0.001	–	0.01
Common $(B^0, \overline{B}^0)$	Mass propagators parameters	0.19	0.031	0.070	0.200	0.018	0.06	0.011	0.005	0.006	0.01	0.01
	Masses and angles resolution	0.02	0.027	0.017	0.026	0.026	0.05	0.010	0.016	0.018	0.14	0.12
	Fit method	–	0.004	0.001	0.002	0.001	–	0.003	0.001	0.002	0.01	0.05
	$a_1(1260)$ pollution	0.09	0.040	0.040	0.040	0.050	0.04	0.015	0.040	0.031	0.02	0.01
	Symmetrised $(\pi\pi)$ PDF	0.03	0.029	0.022	0.035	0.006	0.05	0.004	–	0.004	0.04	0.05

	Systematic uncertainty	$f^{\perp}_{\omega K^*}$	$\delta^{\|\|-\perp}_{\rho K^*}$	$\delta^{\|\|-0}_{\rho K^*}$	$\delta^{\perp-0}_{\rho K^*}$	$\delta^{\|\|-\perp}_{\omega K^*}$	$\delta^{\|\|-0}_{\omega K^*}$	$\delta^{\perp-0}_{\omega K^*}$	$\mathcal{A}_{\mathrm{T}}^{\rho K^*,1}$	$\mathcal{A}_{\mathrm{T}}^{\rho K^*,2}$	$\mathcal{A}_{\mathrm{T}}^{\omega K^*,1}$	$\mathcal{A}_{\mathrm{T}}^{\omega K^*,2}$
CP averages	Centrifugal barrier factors	–	0.001	–	–	–	–	–	0.0002	–	0.001	0.001
	Hypatia parameters	–	0.001	–	–	–	–	–	0.0002	–	0.001	0.001
	$B^0_s \to K^{*0}\overline{K}^{*0}$ bkg.	0.01	0.018	0.02	0.02	0.1	–	0.1	0.0017	0.002	0.004	0.002
	Simulation sample size	0.03	0.009	0.02	0.02	0.2	0.2	0.2	0.0013	0.002	0.012	0.012
	Data-Simulation corrections	–	0.001	–	–	–	–	–	–	–	–	–
CP asym.	Centrifugal barrier factors	–	0.004	0.007	0.004	0.03	0.02	0.04	0.0003	0.001	0.001	0.001
	Hypatia parameters	0.1	0.001	0.002	0.002	0.02	0.01	0.02	0.0001	–	0.001	0.001
	$B^0_s \to K^{*0}\overline{K}^{*0}$ bkg.	0.2	0.024	0.020	0.026	0.06	0.04	0.13	0.0017	0.004	0.005	0.003
	Simulation sample size	0.1	0.011	0.027	0.023	0.14	0.17	0.20	0.0013	0.002	0.015	0.017
	Data-Simulation corrections	–	–	0.002	0.002	0.02	0.01	0.01	–	–	0.001	–
Common $(B^0, \overline{B}^0)$	Mass propagators parameters	–	0.004	0.028	0.024	0.07	0.06	0.09	0.0006	0.001	0.002	–
	Masses and angles resolution	0.08	0.031	0.029	0.040	0.60	0.40	0.60	0.0020	0.005	0.026	0.019
	Fit method	0.03	0.003	0.005	0.004	0.02	0.02	0.03	0.0001	–	0.005	0.001
	$a_1(1260)$ pollution	0.01	0.024	0.035	0.032	0.24	0.32	0.40	0.0040	0.004	0.012	0.001
	Symmetrised $(\pi\pi)$ PDF	0.03	0.005	0.001	0.001	0.35	0.02	0.29	0.0007	0.001	0.018	0.003

$B^0 \to \rho^0 K^{*0}$

Mass fit

- Shapes:
  - Signal: Hypatia distribution with parameters obtained from simulation. The same shape is used for B^0 and B_s^0, except with a mass shift

$B^0 \to K^{*0} \overline{K}^{*0}$

Full Results

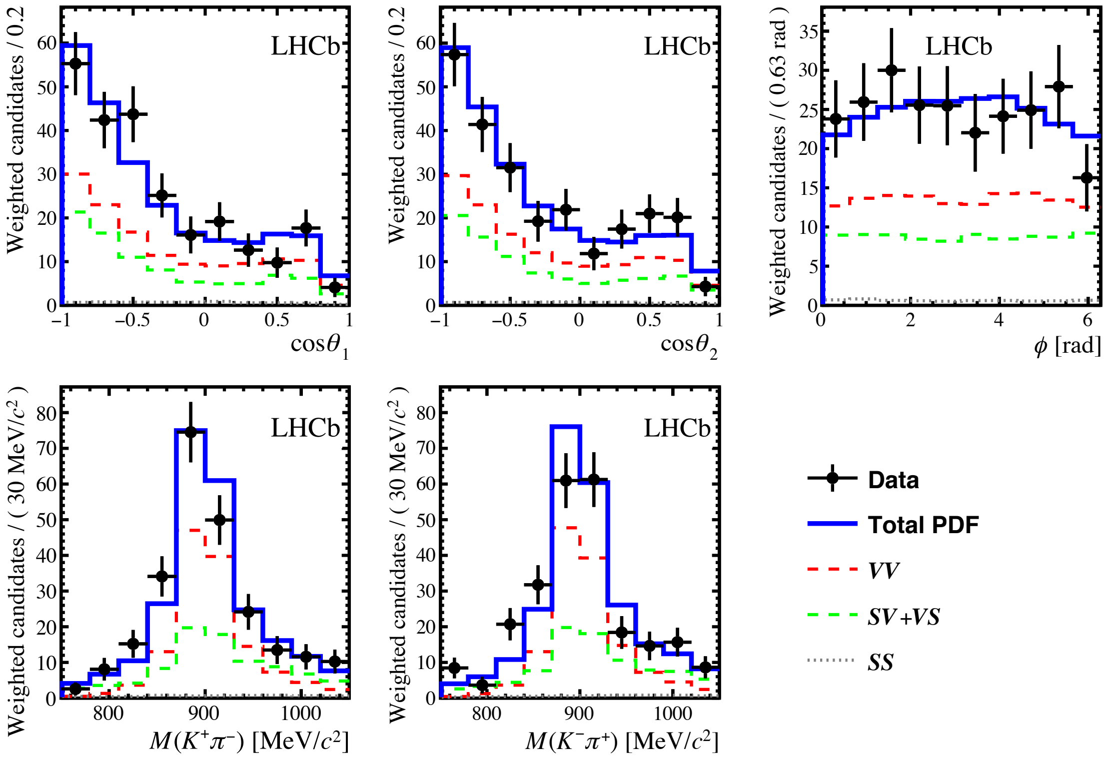

Figure 4: Projections of the amplitude fit results for the $B^0 \to K^{*0}\overline{K}^{*0}$ decay mode on the helicity angles (top row: $\cos\theta_1$ left, $\cos\theta_2$ centre and ϕ right) and on the two-body invariant masses (bottom row: $M(K^+\pi^-)$ left and $M(K^-\pi^+)$ centre). The contributing partial waves: VV (dashed red), VS (dashed green) and SS (dotted grey) are shown with lines. The black points correspond to data and the overall fit is represented by the blue line.

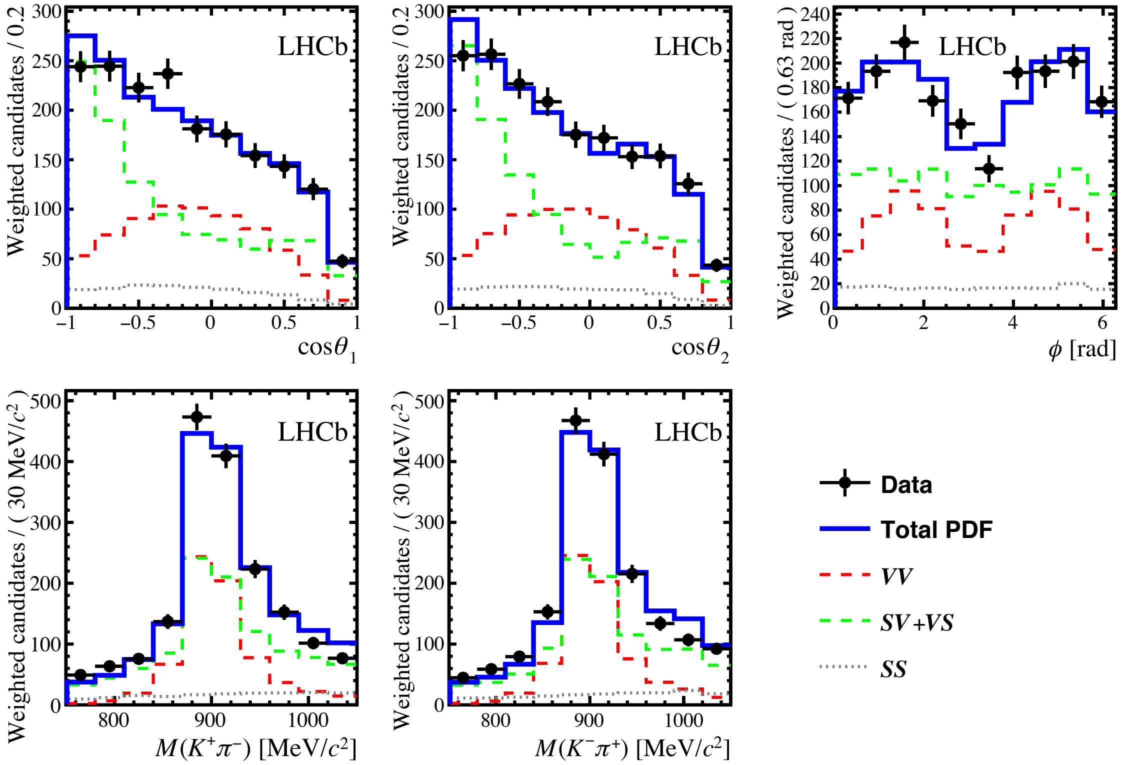

Figure 5: Projections of the amplitude fit results for the $B_s^0 \to K^{*0}\overline{K}^{*0}$ decay mode on the helicity angles (top row: $\cos\theta_1$ left, $\cos\theta_2$ centre and ϕ right) and on the two-body invariant masses (bottom row: $M(K^+\pi^-)$ left and $M(K^-\pi^+)$ centre). The contributing partial waves: VV (dashed red), VS (dashed green) and SS (dotted grey) are shown with lines. The black points correspond to data and the overall fit is represented by the blue line.

$B^0 \to K^{*0} \overline{K}^{*0}$

Full Results

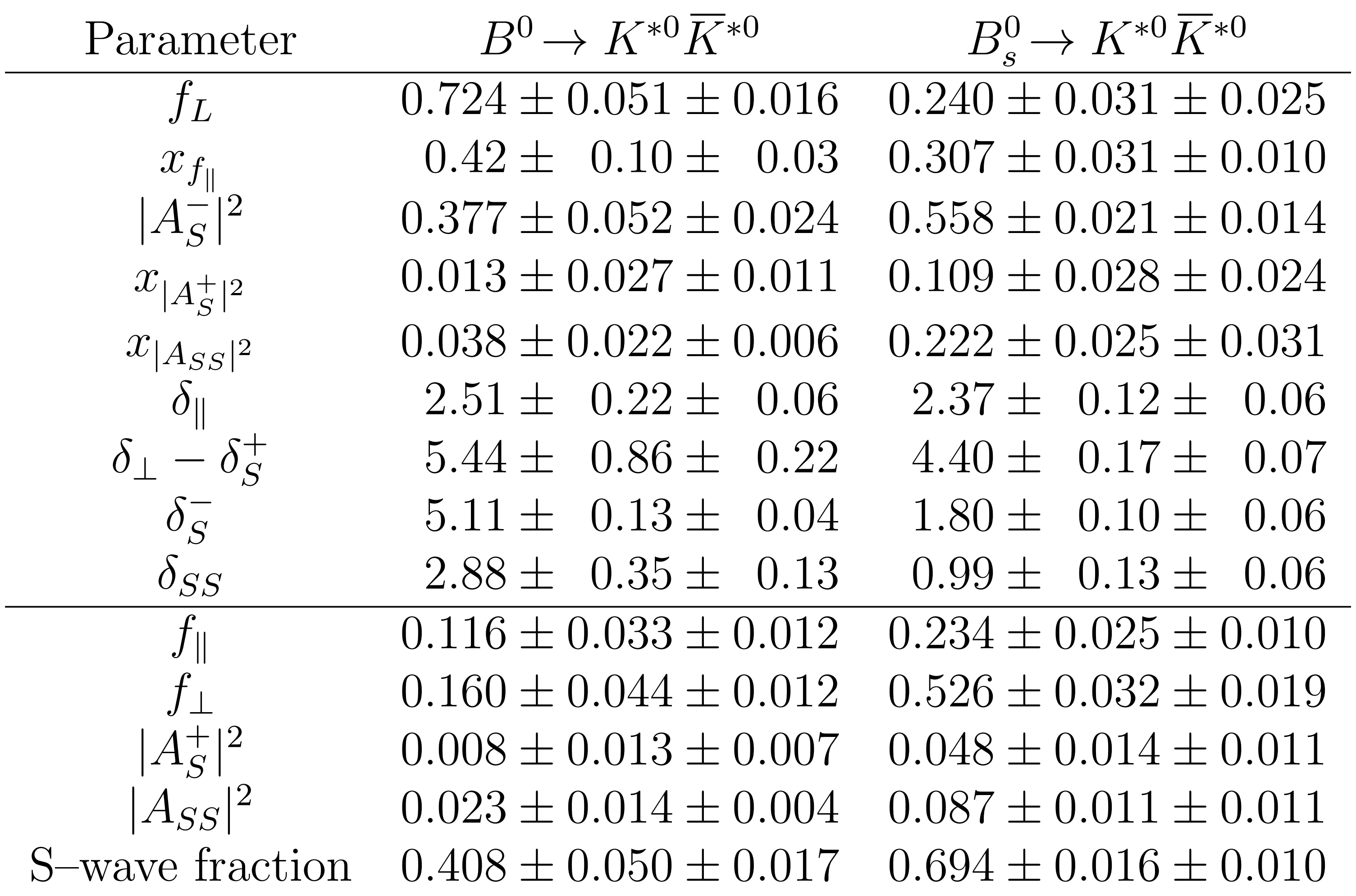

Parameter	$B^0 \to K^{*0}\overline{K}^{*0}$	$B_s^0 \to K^{*0}\overline{K}^{*0}$
f_L	$0.724 \pm 0.051 \pm 0.016$	$0.240 \pm 0.031 \pm 0.025$
$x_{f_\parallel}$	$0.42 \pm 0.10 \pm 0.03$	$0.307 \pm 0.031 \pm 0.010$
$\lvert A_S^-\rvert^2$	$0.377 \pm 0.052 \pm 0.024$	$0.558 \pm 0.021 \pm 0.014$
$x_{\lvert A_S^+\rvert^2}$	$0.013 \pm 0.027 \pm 0.011$	$0.109 \pm 0.028 \pm 0.024$
$x_{\lvert A_{SS}\rvert^2}$	$0.038 \pm 0.022 \pm 0.006$	$0.222 \pm 0.025 \pm 0.031$
$\delta_\parallel$	$2.51 \pm 0.22 \pm 0.06$	$2.37 \pm 0.12 \pm 0.06$
$\delta_\perp - \delta_S^+$	$5.44 \pm 0.86 \pm 0.22$	$4.40 \pm 0.17 \pm 0.07$
δ_S^-	$5.11 \pm 0.13 \pm 0.04$	$1.80 \pm 0.10 \pm 0.06$
δ_{SS}	$2.88 \pm 0.35 \pm 0.13$	$0.99 \pm 0.13 \pm 0.06$
$f_\parallel$	$0.116 \pm 0.033 \pm 0.012$	$0.234 \pm 0.025 \pm 0.010$
$f_\perp$	$0.160 \pm 0.044 \pm 0.012$	$0.526 \pm 0.032 \pm 0.019$
$\lvert A_S^+\rvert^2$	$0.008 \pm 0.013 \pm 0.007$	$0.048 \pm 0.014 \pm 0.011$
$\lvert A_{SS}\rvert^2$	$0.023 \pm 0.014 \pm 0.004$	$0.087 \pm 0.011 \pm 0.011$
S–wave fraction	$0.408 \pm 0.050 \pm 0.017$	$0.694 \pm 0.016 \pm 0.010$

Systematic uncertainties

- Fit method
- Description of kinematic acceptance
- Resolution
- P-wave mass model
- S-wave mass model
- Differences between data and simulation
- Background subtraction
- Peaking backgrounds
- Time acceptance

Branching fraction measurement

- Systematic uncertainties in the factor k
- Systematic uncertainties in the signal yields
- Systematic uncertainties in the efficiencies

Systematic uncertainties

Decay mode	$B^0 \to (K^+\pi^-)(K^-\pi^+)$									$B^0 \to (K^+\pi^-)(K^-\pi^+)$				
Parameter	f_L	$x_{f_\parallel}$	$\|A_S^-\|^2$	$x_{\|A_S^+\|^2}$	$x_{\|A_{SS}\|^2}$	$\delta_\parallel$	$\delta_\perp - \delta_S^+$	δ_S^-	δ_{SS}	$f_\parallel$	$f_\perp$	$\|A_S^+\|^2$	$\|A_{SS}\|^2$	S–wave fraction
Bias data-simulation	0.001	0.00	0.006	−0.001	0.004	0.01	−0.01	0.00	0.01	0.001	−0.001	−0.001	0.002	0.007
Fit method	0.007	0.01	0.011	0.009	0.001	0.00	0.01	0.00	0.02	0.000	0.007	0.005	0.000	0.006
Kinematic acceptance	0.005	0.01	0.006	0.004	0.002	0.03	0.12	0.01	0.04	0.003	0.004	0.001	0.003	0.006
Resolution	0.007	0.00	0.005	0.001	0.002	0.00	0.16	0.00	0.02	0.001	0.003	0.000	0.001	0.006
P–wave mass model	0.001	0.00	0.004	0.001	0.002	0.00	0.01	0.00	0.02	0.000	0.001	0.000	0.001	0.005
S–wave mass model	0.007	0.01	0.016	0.003	0.002	0.03	0.03	0.03	0.02	0.000	0.007	0.002	0.002	0.008
Differences data-simulation	0.004	0.00	0.002	0.001	0.001	0.01	0.01	0.01	0.01	0.001	0.003	0.000	0.001	0.002
Background subtraction	0.002	0.01	0.006	0.001	0.002	0.01	0.06	0.01	0.09	0.005	0.003	0.001	0.001	0.002
Peaking backgrounds	0.009	0.02	0.009	0.003	0.003	0.04	0.06	0.01	0.08	0.010	0.003	0.002	0.002	0.009
Total systematic unc.	0.016	0.03	0.024	0.011	0.006	0.06	0.22	0.04	0.13	0.012	0.012	0.007	0.004	0.017

Decay mode	$B_s^0 \to (K^+\pi^-)(K^-\pi^+)$									$B_s^0 \to (K^+\pi^-)(K^-\pi^+)$				
Parameter	f_L	$x_{f_\parallel}$	$\|A_S^-\|^2$	$x_{\|A_S^+\|^2}$	$x_{\|A_{SS}\|^2}$	$\delta_\parallel$	$\delta_\perp - \delta_S^+$	δ_S^-	δ_{SS}	$f_\parallel$	$f_\perp$	$\|A_S^+\|^2$	$\|A_{SS}\|^2$	S–wave fraction
Bias data-simulation	0.004	0.003	0.007	−0.003	0.021	0.05	0.00	0.05	0.07	0.001	−0.005	−0.002	0.007	0.012
Fit method	0.001	0.000	0.001	0.000	0.000	0.00	0.00	0.00	0.00	0.001	0.001	0.000	0.001	0.001
Kinematic acceptance	0.011	0.006	0.011	0.021	0.009	0.05	0.07	0.05	0.05	0.005	0.009	0.010	0.004	0.004
Resolution	0.002	0.001	0.000	0.002	0.000	0.00	0.00	0.00	0.00	0.000	0.002	0.000	0.001	0.002
P–wave mass model	0.001	0.000	0.001	0.002	0.009	0.00	0.01	0.00	0.01	0.000	0.001	0.001	0.003	0.005
S–wave mass model	0.021	0.001	0.007	0.011	0.028	0.03	0.02	0.03	0.02	0.006	0.016	0.004	0.009	0.006
Differences data-simulation	0.002	0.000	0.001	0.001	0.001	0.01	0.00	0.01	0.01	0.001	0.001	0.000	0.001	0.001
Background subtraction	0.000	0.001	0.001	0.001	0.004	0.01	0.01	0.01	0.01	0.001	0.001	0.001	0.002	0.002
Peaking backgrounds	0.003	0.008	0.002	0.002	0.002	0.02	0.01	0.02	0.01	0.007	0.005	0.001	0.001	0.001
Time acceptance	0.008	0.014	0.008	0.004	0.005	0.00	0.00	0.00	0.00	0.008	0.016	0.003	0.001	0.007
Total systematic unc.	0.025	0.010	0.014	0.024	0.031	0.06	0.07	0.06	0.05	0.010	0.019	0.011	0.011	0.010

$B^0 \rightarrow K^{*0} \overline{K}^{*0}$

Mass fit

- Shapes:
  - Signal: Double-sided Hypatia distributions with the same parameters other than mass difference
  - Mis-ID: sum of a Crystal ball and gaussian with parameters from simulations (except mean and sigma)
  - Part-Reco: ARGUS function convolved with a gaussian resolution function